# ChemComm

Accepted Manuscript

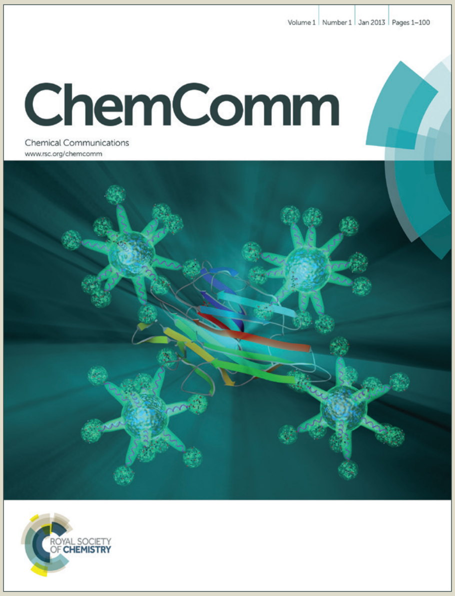

Volume 1 | Number 1 | Jan 2013 | Pages 1–100

ChemComm

Chemical Communications

www.rsc.org/chemcomm

ROYAL SOCIETY
OF CHEMISTRY

www.rsc.org/chemcomm

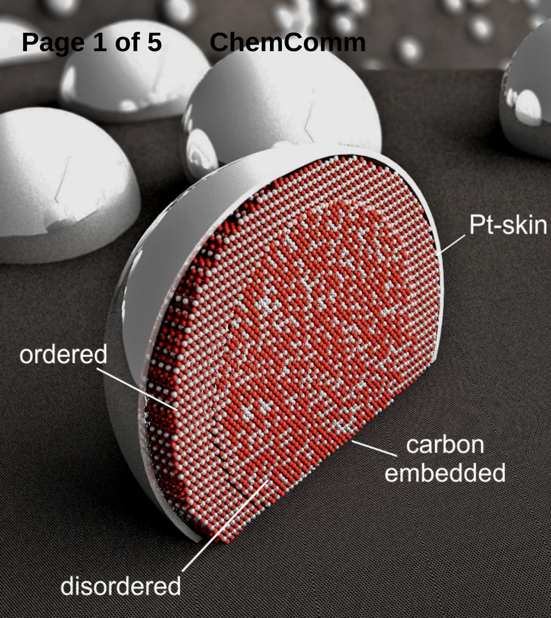
Pt-skin
ordered
carbon embedded
disordered

Journal Name RSCPublishing

COMMUNICATION

Cite this: DOI: 10.1039/x0xx00000x

Received 00th January 2012,
Accepted 00th January 2012

DOI: 10.1039/x0xx00000x

www.rsc.org/

# A highly active $PtCu_3$ intermetallic core-shell, multilayered Pt-skin, carbon embedded electrocatalyst produced by a scale-up sol-gel synthesis

M. Bele,[a] P. Jovanovič,[a] A. Pavlišič,[a] B. Jozinović,[a] M. Zorko,[a] A. Rečnik,[b] E. Chernyshova,[a] S. Hočevar,[c] N. Hodnik [c]* and M. Gaberšček[a]*

**We present a novel, scaled-up sol-gel synthesis which enables one to produce 20 g batches of highly active and stable carbon supported $PtCu_3$ nanoparticles as a cathode material for low temperature fuel cell application. We confirm the presence of ordered intermetallic phase underneath multilayered Pt-skin together with firm embedment of nanoparticles in the carbon matrix.**

Among numerous promising applications for fuel cells, the automotive usage seems to be the crucial one since electrical motors powered by fuel cells offer renewable and non-pollutant replacement for the fossil fuel-based combustion engines. However the efficiency of low temperature fuel cells is still limited by the sluggish kinetics, stability issues and costs of the cathode catalyst for oxygen reduction reaction (ORR). Various catalysts, such as platinum and platinum alloys with and without carbon-based supports as well as catalyst without precious metals have been implemented to reduce the ORR polarisation and achieve a maximum reaction efficiency.[1] Among the materials with highest mass activities are Pt-based catalysts with enhanced activity due to the so-called strain and ligand effects achieved through a d-band centre shift induced by the transition elements.[1-5] The so-called multilayered Pt-skin catalysts [6, 7] are supposed to have a few layers of platinum on a less noble metal rich core. Note that in our manuscript, the term Pt-skin is used to describe a 2–3 atomic-layer-thick platinum shell while the more strict definition proposed by Stamenkovic et al. on single crystalline electrode[3] understands the Pt skin as 1 atomic-layer of platinum with oscillating concentration profile around the bulk composition underneath. The PtCu system has shown exciting results - not just for ORR but also for other reactions like methanol oxidation.[8, 9] Interestingly, additional enhancement of the electrocatalytic activity and stability has been recently shown in the case of C-supported $PtCu_3$ particles where the presence of ordered structure induces significantly higher specific ORR activity and stability compared to the fully disordered sample.[10] In previous studies the enhancement effect of ordering on activity of PtCu system has been mentioned but not directly proven.[11-14] Here we present a novel Pt-skin $PtCu_3$ alloy catalyst with core-shell nanoparticles (intermetallic ordered shell @ a disordered core, as shown in Figure 1) tightly embedded (anchored) into carbon support. Most importantly, the new electrocatalyst was prepared *via* a scaled-up procedure (up to 20 g in one batch) based on modified sol-gel synthesis using a gelatin precursor. The new catalyst highly outperforms the conventional Pt benchmark (3 nm Pt nanoparticles on high surface area carbon) and markedly exceeds the US Department of Energy target: the specific activity of 0.7 $mA/cm^2_{Pt}$ exceeds the 2017 DOE target by 350 % while the mass activity of 0.44 $A/mg_{Pt}$ exceeds the DOE 2015 goal by 250 % (Table 1).[1] Very importantly, it also exhibits a 50 % decreased Pt dissolution compared to the same conventional Pt 3 nm benchmark electrocatalyst under potentiodynamic treatment.[15]

The synthesis was directed towards achieving the following major goals: the presence of Pt-skin, the presence of ordered intermetallic phase, firm embedment into carbon and possibility of large-scale production. Detailed discussion of the activity enhancement supported with DFT calculations as well as extensive description of the processes taking place during the synthesis will be presented in forthcoming full papers. Essential information regarding the synthesis and preparation of this and other new electrocatalysts can be found in ref [8, 16] and in a recent US patent application[17] however note that they do not fully refer to the present scaled-up version. In general, the present synthesis consists of 5 steps: xerogel preparation, pyrolysis, platination, partial oxydation and annealing. After the xerogel and pyrolysis steps, pure copper particles are already completely embedded in a carbon matrix (a combination of amorphous pyrolytic gelatin-derived carbon and graphitic Vulcan XC72). After that, platinum is added *via* a galvanic replacement process followed first by partial oxidation in order to burn off the excessive carbon and then by the annealing procedure in reducing atmosphere. Due to direct nucleation and growth on proper carbon precursors, an intimate junction between the carbon and the alloyed nanoparticles is established. The annealing (15 min 750 °C followed by 1 hour at 500 in 5 % $H_2$-Ar) crucially affects at least three material's features: 1. particle size distribution [11] (in our case the mean size is 20-30 nm), 2. intermetallic ordering in the particles' shells, whereas the core might remain kinetically still in the form of copper-platinum solid solution, and 3. Pt segregation to the surface (Pt-skin formation).[3] The overall chemical composition of the present catalyst materials was ca. 20 wt. % of platinum, 20 wt. % of copper, the rest being carbon.

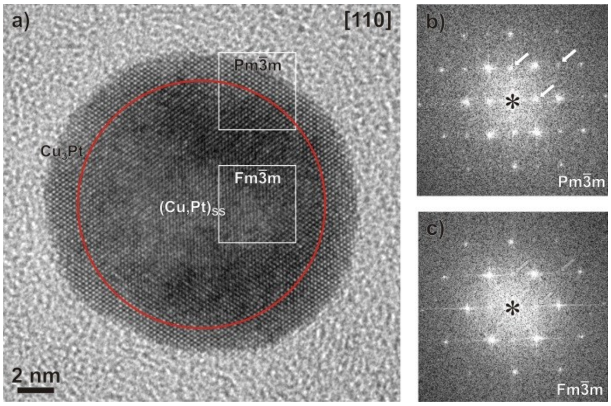

***Figure 1.*** a) Cross-section HRTEM image of a single $PtCu_3$ nanoparticle crystal oriented along the crystallographic [11-0] axis showing an apparent core-shell ordered-disordered structure of the present catalyst. Averaged FFT power spectra for the shell and core regions are shown in (b) Pm3-m with extra reflections (marked with arrows) and (c) Fm3-m without the super-structure reflections.

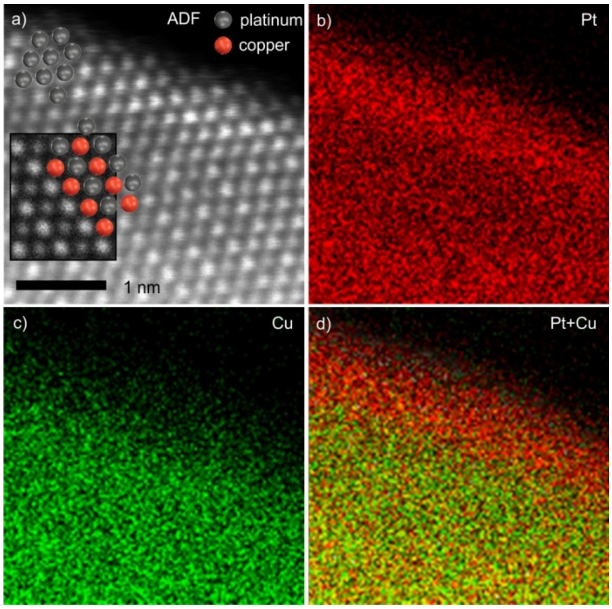

***Figure 2.*** a-d) Direct evidence of Pt-skin formation on the surface of catalyst particles. The atomic columns with a brighter contrast at the STEM-HAADF image (a) correspond to Pt, the insert shows a simulated $PtCu_3$ ordered structure. This phase was observed at the outer edge of the particle, which finished with the Pt-skin of a thickness of below 1nm formed at a very surface of the particle. The skin is clearly visible in EDX maps (b-d), acquired simultaneously with HAADF-STEM image.

A systematic comparison of large number of differently synthesized PtCu catalysts has shown that the catalysts possessing a significant amount of ordered Pm3-m phase outperformed the alloys possessing merely the disordered Fm3-m structure by at least 20-30% [10] and in some samples even up to 300% in specific activity. Detailed analysis of selected particles showed that the ordered phase always formed a shell around the disordered core (Figure 1) – reflecting the surface-to-core phase growth during the annealing procedure. Furthermore, consistently with previous reports on similar alloy systems,[6, 7] the existence of a Pt-skin can be demonstrated on the surface of particles (Figure 2). Finally, for better stability tight embedment into carbon support (Figure 3) is also crucial. It prevents particles to migrate, detach and agglomerate.[18]

***Table 1.*** RDE ORR activity data measurements

| RDE | $j_k$ [a]<br>$mA/cm^2_{Pt}$ | $j_m$ [b]<br>$A/mg_{Pt}$ | ESA<br>$m^2/g_{Pt}$ |
|---|---|---|---|
| $PtCu_3/C$ | 2.5 | 1.1 | 45 |
| Pt/C | 0.27 | 0.2 | 73 |

[a] specific activity at 0.9 $V_{RHE}$ [b] mass activity at 0.9 $V_{RHE}$

The present $PtCu_3/C$ catalyst outperforms other de-alloyed $Pt_xCu_y/C$ and $Pt_xCo_y/C$ by at least a factor of 2.[1] Therefore, we assume that some additional effects besides Pt-skin and ordered phase could be beneficial for the high ORR activity as indicated in continuation.

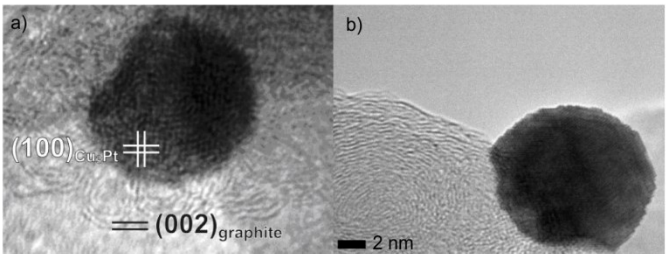

*Figure 3.* a,b) Semi-epitaxial growth of lacey, graphene-like bands sprouting from the 8 nm large CuPt particle oriented close to the [001] zone axis are concave imprints on some crystals (the visibility of the imprints depends on the crystal orientation) at the original attachment point with carbon matrix.

From the Tafel plots shown in Figure 4b it is seen that the ordered catalyst outperforms the Pt benchmark as well as the disordered one by a factor of 10 and 2, respectively, in mass activity. As mentioned, the high specific activity can to some extent be explained by the existence of a Pt-skin[6, 7] the presence of which was not only detected by STEM-HAADF and EDX mapping (Figure 2 b-d) but also confirmed by the $Q_{CO}/Q_{Hupd}$ ratio of 1.4.[7] The second factor leading to the enhancement of activity is the phase ordering[10] which in the present case increases the activity at least by a factor of two (compare the activities of the ordered and disordered alloy in Figure 4). Thirdly, the convenient particle size from 5 to 30 nm (in our specific case the mean value was between 20-30 nm) is known to enhance the activity by a factor of two due to the nanoparticles size effect.[19] Finally, the effect of support, which is known in the heterogeneous catalysis as SMSI (strong metal-support interaction [20]) should not be neglected. Namely, C-based non-noble materials alone can also act as good ORR catalyst. It could be that the very tight embedment of our alloyed nanoparticles into C additionally enhances the overall activity through combined or even synergistic Pt-C action. This possibility needs to be explored further.

It should be noted that better catalysts for ORR have been demonstrated previously, such as nanostructured thin-films (NSTF) and shape/size controlled nanoparticles which exhibit very high specific (from 2 to almost 7 mA/cm$^2_{Pt}$) and mass activities (from 0.3 to 1.5 A/mg$_{Pt}$).[1] However, as pointed out in a recent review article,[1] most of those high performance catalysts are either prepared in (very) small amounts or in a form that is inappropriate for testing in fuel cell environment. By contrast the present material, the RDE activity of which is the best so far found for a PtCu catalyst, can be prepared in quantities of at least 20 g per batch. This catalyst is also very stable: the ESA does not change from the initial value of about 45 m$^2$/g$_{Pt}$ even after 7000 potential cycles between 0.47 V and 1.07 V scanned with 1 V/s in 0.1 M $HClO_4$. However, it needs to be noted that in a real low temperature fuel cell any leached Cu might be transported through the membrane thus contaminating the anode [21].

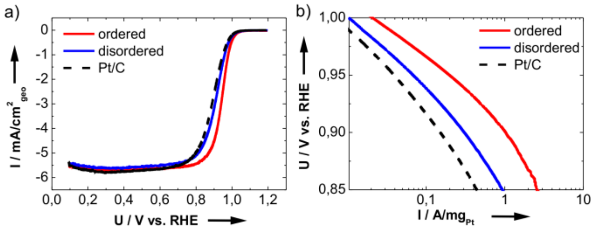

***Figure 4.*** a) ORR polarization curves for Pt benchmark, disordered and ordered $PtCu_3$ catalysts (measured with 20 mV/s at room temperature in $O_2$ saturated 0.1 M $HClO_4$ with Pt loading of approximately 25 µg/cm$^2_{geom}$). b) Tafel plots.

## Conclusions

In conclusion, we have introduced a new, highly active $PtCu_3$ catalyst synthesized using a novel approach that integrates various elements for preparation of high performance, new generation practical electrocatalysts: (i) appropriate thermal annealing induces intermetallic ordering and a Pt-skin, both beneficial for activity of alloyed catalysts[10]; (ii) xerogelation and partial oxidation are responsible for the firm and intimate embedment of alloy into the heterogeneous carbon matrix that provides superior stability and maximized transport of electrons to the active sites; (iii) the synthesis is appropriate for large scale production of the novel $PtCu_3$ catalyst and can easily be extended to other Pt-M alloys. The present catalyst exceeds the DOE 2017 target specific activity of 0.7 mA/cm$^2_{Pt}$ by 350 % and the DOE 2015 target for mass activity of 0.44 A/mg$_{Pt}$ by 250 %. The mass activity could, however, be even further increased by increasing the ESA.

## Notes and references

[a] Laboratory for Materials Chemistry, National Institute of Chemistry Hajdrihova 19, 1000 Ljubljana, Slovenia.
[b] Department for Nanostructured Materials, Jozef Stefan Institute, Ljubljana, 1000, Slovenia.
[c] Laboratory of Catalysis and Chemical Reaction Engineering, National Institute of Chemistry Hajdrihova 19, 1000 Ljubljana, Slovenia.

1. M. K. Debe, *Nature*, 2012, **486**, 43-51.
2. V. Stamenkovic, B. S. Mun, K. J. J. Mayrhofer, P. N. Ross, N. M. Markovic, J. Rossmeisl, J. Greeley and J. K. Nørskov, *Angewandte Chemie International Edition*, 2006, **45**, 2897-2901.
3. V. R. Stamenkovic, B. Fowler, B. S. Mun, G. Wang, P. N. Ross, C. A. Lucas and N. M. Marković, *Science*, 2007, **315**, 493-497.
4. P. Strasser, S. Koh, T. Anniyev, J. Greeley, K. More, C. Yu, Z. Liu, S. Kaya, D. Nordlund, H. Ogasawara, M. F. Toney and A. Nilsson, *Nature chemistry*, 2010, **2**, 454-460.
5. I. E. L. Stephens, A. S. Bondarenko, U. Gronbjerg, J. Rossmeisl and I. Chorkendorff, *Energy & Environmental Science*, 2012, **5**, 6744-6762.
6. D. F. van der Vliet, C. Wang, D. Li, A. P. Paulikas, J. Greeley, R. B. Rankin, D. Strmcnik, D. Tripkovic, N. M. Markovic and V. R. Stamenkovic, *Angewandte Chemie International Edition*, 2012, **51**, 3139-3142.
7. N. Hodnik, M. Bele and S. Hočevar, *Electrochemistry Communications*, 2012, **23**, 125-128.
8. N. Hodnik, M. Bele, A. Rečnik, N. Z. Logar, M. Gaberšček and S. Hočevar, *Energy Procedia*, 2012, **29**, 208-215.
9. X. Yu, D. Wang, Q. Peng and Y. Li, *Chemical Communications*, 2011, **47**, 8094-8096.
10. N. Hodnik, C. Jeyabharathi, J. C. Meier, A. Kostka, K. L. Phani, A. Recnik, M. Bele, S. Hocevar, M. Gaberscek and K. J. J. Mayrhofer, *Physical Chemistry Chemical Physics*, 2014, **16**, 13610-13615.
11. D. Wang, Y. Yu, H. L. Xin, R. Hovden, P. Ercius, J. A. Mundy, H. Chen, J. H. Richard, D. A. Muller, F. J. DiSalvo and H. D. Abruña, *Nano Letters*, 2012, **12**, 5230-5238.
12. I. Dutta, M. K. Carpenter, M. P. Balogh, J. M. Ziegelbauer, T. E. Moylan, M. H. Atwan and N. P. Irish, *The Journal of Physical Chemistry C*, 2010, **114**, 16309-16320.
13. B. Y. Xia, H. B. Wu, X. Wang and X. W. Lou, *Journal of the American Chemical Society*, 2012, **134**, 13934-13937.
14. C. Jeyabharathi, N. Hodnik, C. Baldizzone, J. C. Meier, M. Heggen, K. L. N. Phani, M. Bele, M. Zorko, S. Hocevar and K. J. J. Mayrhofer, *ChemCatChem*, 2013, **5**, 2627-2635.
15. P. Jovanovič, A. Pavlišič, V. S. Šelih, M. Šala, N. Hodnik, M. Bele, S. Hočevar and M. Gaberšček, *ChemCatChem*, 2014, **6**, 449-453.
16. N. Hodnik, M. Zorko, M. Bele, S. Hočevar and M. Gaberšček, *The Journal of Physical Chemistry C*, 2012, **116**, 21326-21333.
17. M. Bele, M. Gaberšček, G. Kapun, N. Hodnik and S. Hočevar, *Electrocatalytic Composite(s), Associated Composition(s) and Associated Process(es): Patent application : US Appln*, United States Patent and Trademark Office, 2011.

18. J. C. Meier, C. Galeano, I. Katsounaros, A. A. Topalov, A. Kostka, F. Schüth and K. J. J. Mayrhofer, *ACS Catalysis*, 2012, **2**, 832-843.
19. M. Nesselberger, S. Ashton, J. C. Meier, I. Katsounaros, K. J. J. Mayrhofer and M. Arenz, *Journal of the American Chemical Society*, 2011, **133**, 17428-17433.
20. C. T. Campbell, *Nat Chem*, 2012, **4**, 597-598.
21. Z. Yu, J. Zhang, Z. Liu, J. M. Ziegelbauer, H. Xin, I. Dutta, D. A. Muller and F. T. Wagner, *The Journal of Physical Chemistry C*, 2012, **116**, 19877-19885.